Stalkup, F. I., and H. A. Deans, "Perturbation Velocities in Gas-Liquid Partition chromatographic Columns, *AIChE J.*, **9**, 106 (1963).
Valentin, P., and G. Guiochon, "Determination of Gas-Liquid and Gas-Solid Equilibrium Isotherms by Chromatography: I. Theory of the Step-and-Pulse Method," *J. of Chromat. Sci.*, **14**, 56 (1976).
Zhukhovitskii, A. A., N. M. Turkel'taub, L. A. Malyasova, A. F. Shlyakhov, V. V. Naumova, and T. I. Pogrebnaya, "Chromatography Without a Carrier-Gas," *Indus. Lab.*, **29**, 1273 (1963).
Zhukhovitskii, A. A., M. L. Sazonov, A. F. Shlyakhov, and A. I. Karymova, "Development Chromatography Without a Carrier Gas," *Indus. Lab.*, **31**, 1301 (1965).
Zhukhovitskii, A. A., M. L. Sazonov, A. F. Shlyakhov, and V. P. Shvartsman, "Theory of Chromatography Without Carrier Gas," *Russian J. of Phys. Chem.*, **41**, 1429 (1967).

Manuscript received October 15, 1981; revision received March 29, and accepted April 19, 1982.

Effect of the Product Layer on the Kinetics of the CO_2-Lime Reaction

The kinetics of reaction between CO_2 and lime is investigated in the range of 673 to 998 K with a view to examining the effects of product layer deposition and variations in the limestone calcination atmosphere. The reaction is initially rapid and chemically controlled and goes through a sudden transition to a much slower regime controlled by diffusion in the product $CaCO_3$ layer. The magnitude of the estimated product layer diffusivity is in the range of 10^{-18} to 10^{-21} m^2/s, the corresponding activation energy is 88.9 ± 3.7 kJ/mol below 688 K and 179.2 ± 7.0 kJ/mol above that temperature, suggestive of solid state diffusion. Plausible mechanisms are discussed.

S. K. BHATIA and D. D. PERLMUTTER
Department of Chemical Engineering
University of Pennsylvania
Philadelphia, PA 19104

SCOPE

The effect of pore structure and the influence of product layer diffusion on the CO_2-lime reaction has been examined in the temperature range of 673 to 998 K under CO_2 levels varying from 10 to 42% in nitrogen. The data is analyzed by means of the random pore model (Bhatia and Perlmutter, 1980, 1981a), and intrinsic rate constants as well as product layer diffusion coefficients are determined. Product layer diffusion coefficients for calcines prepared under varying levels of CO_2 in nitrogen are compared, and the role of solid state processes in the product layer diffusion process is examined.

CONCLUSIONS AND SIGNIFICANCE

Analysis of kinetics data indicates that after nucleation is complete at about 12% conversion the CaO-CO_2 reaction proceeds by a rapid surface reaction-controlled step, followed by a slower second stage product layer diffusion-controlled process. The high activation energy for product layer diffusion (88.9 kJ/mol below 688 K and 179 kJ/mol above 688 K) and the low values of the effective diffusitivity (10^{-18} to 10^{-22} m^2/s) are suggestive of a solid state diffusion. Calcines with different surface areas prepared under CO_2-containing atmospheres show agreement in the estimated product layer diffusivity. The values for the calcines prepared under nitrogen are however different, indicating variations in defect structure.

The bulk of the pores in all the calcines lie in a narrow size range with a small amount of porosity distributed among larger pores. Over most of the conversion range the smaller pores dominate reaction, but at about 60% conversion the pores in this narrow size range appear to close because the molar volume of $CaCO_3$ far exceeds that of CaO. Further conversion is thus restricted to the much larger pores which react only slowly. The incomplete conversions obtained for this reaction in this study and those of Nitsch (1962), Dedman and Owen (1962), and Barker (1973, 1974) may be attributed to this phenomenon.

The literature reports many studies of the kinetics of the decomposition of calcium carbonate (Zawadzki and Betsznajder, 1935; Hyatt et al., 1958; Cremer and Nitsch, 1962; Beruto and Searcy, 1974; Searcy and Beruto, 1976), but less attention has been paid to the reverse reaction:

$$CaO\,(s) + CO_2\,(g) \rightleftharpoons CaCO_3\,(s)$$

This reaction is of practical significance in the CO_2 acceptor process for coal gasification, and in the synthesis of calcium cyanamide (Dedman and Owens, 1962). Further, it has recently been suggested as an attractive candidate reaction for consideration in energy storage (Barker, 1973, 1974). This paper reports experimental kinetics for this reaction and applies the random pore model (Bhatia and Perlmutter, 1980, 1981a) to interpret the data.

The prior studies of Nitsch (1962), Dedman and Owen (1962), and Barker (1973, 1974) on the recarbonation of lime indicate a relatively rapid initial reaction followed by a much slower second stage. Nitsch (1962) found that the initial growth stage reaction rate in the temperature range of 1073 to 1123 K could be correlated by

$$\frac{dX}{dt} = k_x\,(1 - X)^{2/3}\,(C - C_e) \qquad (1)$$

0001-1541-83-6069-0079$2.00.

where C_e is the equilibrium concentration of carbon dioxide. This first order reversible representation for the effect of CO_2 concentration is also consistent with the prior reports of Zawadzki and Bretsznajder (1935), and Zawadzki (1950) for temperatures above 973 K. Nitsch (1962) also observed that the rate constant k_x in Eq. 1 has a zero activation energy, consistent with related claims (Zawadzki and Bretsznajder, 1935; Cremer and Nitsch, 1962) that the reverse decomposition reaction has an activation energy equal to the heat of dissociation.

Several authors (Nitsch, 1962; Dedman and Owen, 1962; Barker 1973, 1974) report that the reaction does not go to complete conversion. Nitsch found ultimate conversions in the range of 70 to 80%. Both Nitsch, and Dedman and Owen found the slower second stage to be independent of gas composition below 873 K, and independent of CO_2 partial pressures above 1.34 kPa. They attribute this stage to a diffusional process but offer no descriptive kinetic laws. Dedman and Owen (1962) calculated an activation energy of 39.9 ± 8.4 kJ/mol from estimated reaction rates. This apparent value would be about half the true activation energy, if a strong diffusional resistance existed; hence the true value should be estimated as 79.8 ± 16.8 kJ/mol. This result is much too high to be consistent with their speculation that diffusion of CO_2 gas in the pores is controlling the overall process. Further, if diffusion of CO_2 were the controlling factor, the rate would be dependent on CO_2 partial pressure, in contradiction to the experimental finding.

It should be noted that Eq. 1 used by Nitsch (1962) is identical with the spherical grain model of Szekely et al. (1976), if the effective rate constant k_x is expressed as

$$k_x = \frac{k_s S_o}{(1 - \epsilon_o)} \tag{2}$$

to allow for the effects of internal surface area. Limes with wider pores generally have smaller surface areas and react more slowly (Borgwardt and Harvey, 1972; Ulerich et al., 1978), but show higher ultimate conversion (Ulerich et al., 1978). There is therefore a trade-off to be considered in choosing the proper conditions for limestone calcination, since the choice of conditions is known to influence the pore structure of the lime produced (Mullins and Hatfield, 1970; McClellan and Eades, 1970; Ulerich et al., 1978).

Bhatia and Perlmutter (1980, 1981a) and Gavalas (1980) have developed random pore models to correlate reaction behaviour with the internal pore structure. In the regime of reaction control the conversion for a reversible first order system is given by

$$\frac{1}{\psi}\left[\sqrt{1 - \psi \ln (1 - X)} - 1\right] = \frac{k_s S_o (C - C_e) t}{2(1 - \epsilon_o)} \tag{3}$$

to account for the internal pore structure in terms of the surface area S_o, porosity ϵ_o, and the structural parameter defined by

$$\psi = \frac{4\pi L_o (1 - \epsilon_o)}{S_o^2} \tag{4}$$

By taking into account pore intersections Gavalas (1980) has shown that the parameters S_o and L_o may be calculated from mercury porosimetry data through the equations

$$S_o = 2(1 - \epsilon_o) \int_o^\infty \frac{dv_o}{r(1 - v_o)} \tag{5}$$

and

$$L_o = (1 - \epsilon_o) \int_o^\infty \frac{dv_o}{\pi r^2 (1 - v_o)} \tag{6}$$

Bhatia and Perlmutter (1981a) have also derived a rate expression for the instantaneous local reaction rate applicable in the presence of a product layer diffusional resistance:

$$\frac{dX}{dt} = \frac{k_s S_o C_s (1 - X)\sqrt{1 - \psi \ln (1 - X)}}{(1 - \epsilon_o)\left[1 + \frac{\beta Z}{\psi}\left(\sqrt{1 - \psi \ln (1 - X)} - 1\right)\right]} \tag{7}$$

In the limit of product layer diffusion control, (k_s/D_p) and therefore $\beta \to \infty$ and Eq. 7 integrates to the limiting form

TABLE 1. CHEMICAL ANALYSIS OF QUINCY LIMESTONE*

Constituent	wt. %
Calcium Carbonate ($CaCO_3$)	97.73
Calcium (Ca)	39.09
Magnesium Carbonate ($MgCO_3$)	1.47
Silica and Silicates (SiO_2)	0.60
Aluminum and Iron Oxides (R_2O_3)	0.15
Moisture (H_2O)	<0.10
Arsenic (As)	<0.00005
Fluorine (F)	<0.0025
Lead (Pb)	<1.0 ppm
Mercury (Hg)	<0.05 ppm

* Supplied by the Calcium Carbonate Co.

$$\frac{1}{\psi}\left[\sqrt{1 - \psi \ln (1 - X)} - 1\right] = \sqrt{\frac{bMDS_o^2 C_s t}{2a\rho Z(1 - \epsilon_o)^2}} = \frac{S_o}{(1 - \epsilon_o)}\sqrt{\frac{D_P t}{2Z}} \tag{8}$$

EXPERIMENTAL

Sample Preparation

Limestone for these experiments was obtained from the Calcium Carbonate Company of Quincy, Illinois. The detailed composition of the stone, as provided by the supplier, is reported as Table 1. The as-received chips were crushed and screened to two narrow size ranges of −170 +200 U.S. mesh and −100 +120 U.S. mesh.

Calcium oxide was freshly produced for each experiment by decomposing the limestone under a pre-chosen atmosphere in a Dupont Model 951 Thermogravimetric Analyzer (TGA). Each sample was heated to 1,183 K at 20 K/min to effect complete decomposition, held isothermally for 10 minutes under the selected calcining atmosphere, and cooled under N_2 with a controlled temperature program. Limes with three different pore structures were produced by calcination under either (i) pure nitrogen, (ii) nitrogen diluted by 10% CO_2, or (iii) nitrogen diluted by 20% CO_2. These oxides are identified as calcines number 1, 2, and 3, respectively. The individual pore size distribution curves for these calcines were obtained by mercury penetration porosimetry (Micromeritics Model 910 porosimeter) and are shown as Figure 1. It may be noted that the pores are widened and the distribution narrowed as the level of CO_2 is increased in the calcining atmosphere. Correspondingly, the surface area would be expected to decrease. The experimental distribution curves were used to determine the porosities ϵ_o, as well as the surface areas S_o and the total pore lengths L_o via the integrations of Eqs. 5 and 6. In turn these parameters were used to find the structural parameter ψ from Eq. 4. The resulting pore characterizations are presented in Table 2, showing the expected decrease in surface area, and the decrease in ψ noted by Bhatia and Perlmutter (1981b) as characterizing a less-dispersed pore size distribution. For comparison, $\epsilon_o = 0.54$ is the theoretical maximum porosity for CaO of crystal density 3.32

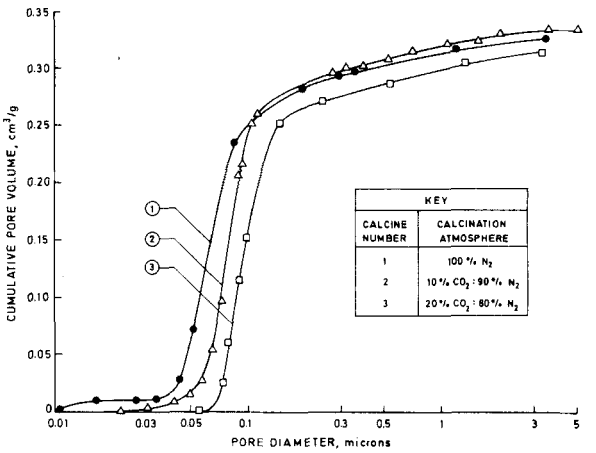

Figure 1. Pore size distributions for several different calcines.

TABLE 2. PORE STRUCTURE PARAMETERS FOR VARIOUS CALCINES

Calcine Number	Calcination Atmosphere	Porosity ϵ_o	Surface Areas, S_o (m^2/cm^3)	Pore Structure Parameter, ψ
1	N_2	0.52	25	2.1
2	10%CO_2-90%N_2	0.53	19	1.6
3	20%CO_2-80%N_2	0.51	14	1.6

g/cm^3 obtained from a non-porous $CaCO_3$ of density 2.71 g/cm^3. X-ray diffraction studies of these materials showed the N_2-produced calcine number 1 to be less crystalline than calcine number 3 prepared under a 20% CO_2–80% N_2 mixture, as evidenced by the sharper CaO peaks, and better splitting of the α_1 and α_2 peaks for the latter calcine. This difference in degree of crystallinity may produce differences in defect structures in the carbonate layers formed on subsequent recarbonation.

Kinetic Measurements

Reaction rates were determined in the same preheated TGA apparatus immediately following the sample preparation by introducing a flow of CO_2/N_2 mixture at a predetermined concentration level in the range of 2 to 42% CO_2. Reaction was followed by the automatic record of weight gain. Results were found to be independent of sample size below 1.3 mg. All gasses were 99.999% pure, as supplied by Airco, Inc.

Because of the prior reports of a metastable oxide (Rao et al., 1960; Beruto and Searcy, 1976) the experiments used either of two different temperature programs to arrive at the isothermal reaction. Samples are designated as having thermal history A, if they were cooled directly to reaction temperature from their preparation at 1,183 K. If the sample was initially cooled to 773 K and then rapidly heated to reaction temperature, it is identified as having thermal history B.

RESULTS

Overall Characteristics

In several respects the CO_2-lime reaction exhibits behavior typical of gas-solid reactions. The data reported as Figures 2 and 3 are, for example, similar to the sigmoid-shaped conversion curves presented by Young (1966), generally interpreted as reflecting an initial nucleation (induction or acceleratory) period, a rapid (growth) reaction, and a slower second stage reaction at higher conversions. Extension of the measurements for 30 minutes beyond the data shown in Figures 2 and 3 confirmed that reaction virtually ceased in the range of 70 to 72% conversion at even the highest temperature of this study, producing a relatively brief second stage reaction. The results in Figure 3 show a somewhat slower nucleation than in Figure 2, indicative of some recrystallization of the lime during the cooling and reheating periods of thermal history B. The slopes of the main growth state are however similar for the two histories at any given temperature, indicating that any surface

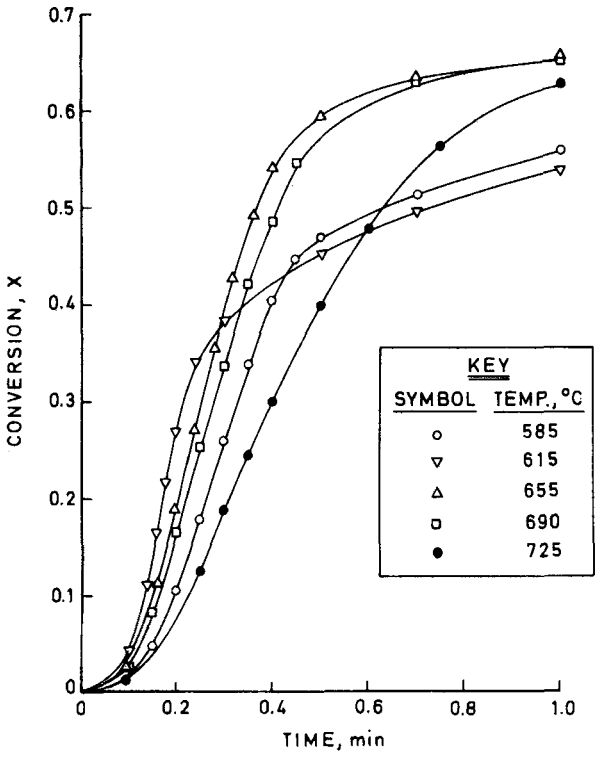

Figure 2. Effect of temperature on reaction of 81 μm (−170 +200 mesh) particles in a 10% CO_2-90% N_2 mixture. Calcine number 1, thermal history A.

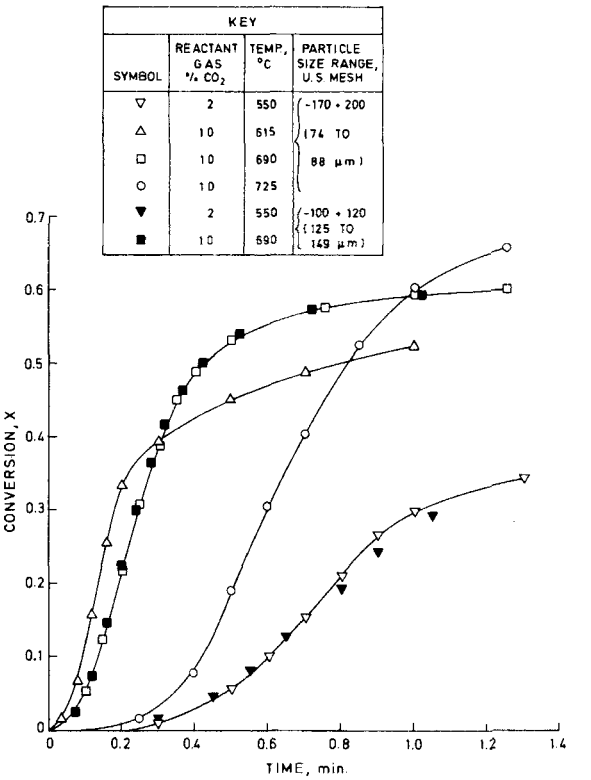

Figure 3. Effect of temperature, gas composition, and particle size on reaction of calcine number 1, thermal history B.

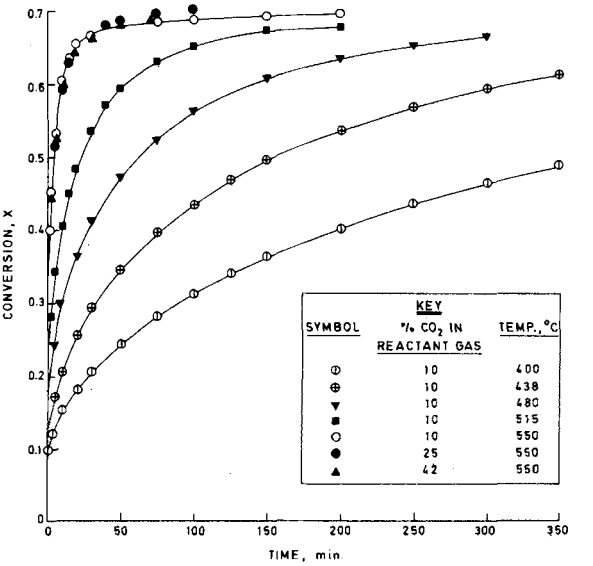

Figure 4. Effect of temperature and gas composition on reaction of 137 μm (−100 +120 mesh) particles. Calcine number 1, thermal history A.

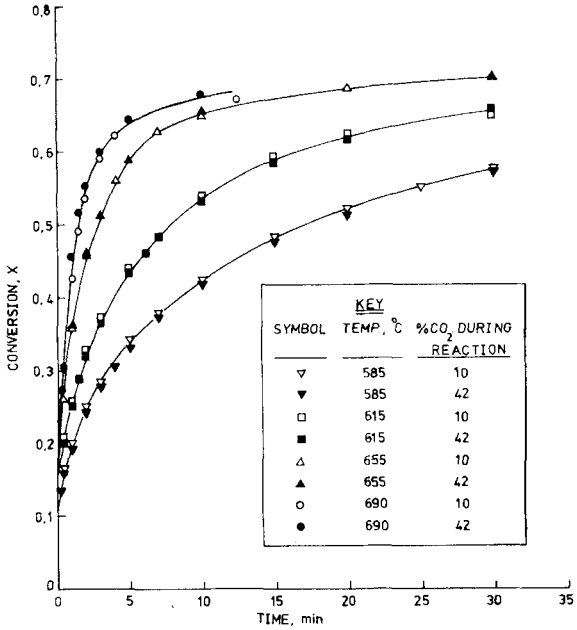

Figure 5. Effect of temperature and gas composition on the reaction of 81 μm (−170 +200 mesh) particles. Calcine number 2, thermal history A.

area changes that occur during the recrystallization are not significant.

The time scale for study can be increased over 100-fold by reducing reaction temperature to the range of 673 to 823 K. As shown in Figure 4, the result is a greatly expanded second-stage reaction that dominates most of the conversion range, but retains the sharply limited maximum conversion at about 70%. A qualitatively similar effect was produced without reduction in reaction temperature by altering instead the conditions under which the lime particles are formed. The results shown in Figures 5 to 8 are for calcines number 2 and 3 produced under gas atmospheres in which the nitrogen had been diluted with 10% and 20% CO_2, respectively. The slower reaction is attributable to the decrease in surface area and increase in pore sizes that were noted above to arise from the calcination in a CO_2-containing atmosphere.

Effect of Particle Size

No significant effect of particle size was noticed under the conditions used in this study. Figure 3 shows that increasing particle size from an average of 81 μm (−170 +200 U.S. mesh) to 137 μm (−100 +120 U.S. mesh) has only negligible effect on the rapid initial stage at both extremes of the temperature range examined. The Figure 9 results for calcine number 2 show as well no significant particle size effect for the second stage reaction. Other runs at 823 K on calcine number 1 confirmed the lack of a particle size effect for the second stage (Bhatia, 1981). It may be concluded that reaction occurs uniformly throughout the solid under the conditions of this work, and as a result that kinetic parameters unaffected by intraparticle and boundary layer diffusion may be evaluated from the data.

Effect of Reaction Gas Composition

It is to be expected that reactant gas concentration can have a different effect on reaction rate, depending on the relative importance of chemical and diffusional contributions. To be consistent with the results of Nitsch (1962) growth stage rates should correlate with reversible first order kinetics. Equation 3 suggests a linearity test for this expectation on coordinates of concentration against a relative rate expressed by:

$$\frac{d}{dt}\left[\frac{\sqrt{1-\psi\,ln\,(1-X)}-1}{\psi}\right]$$

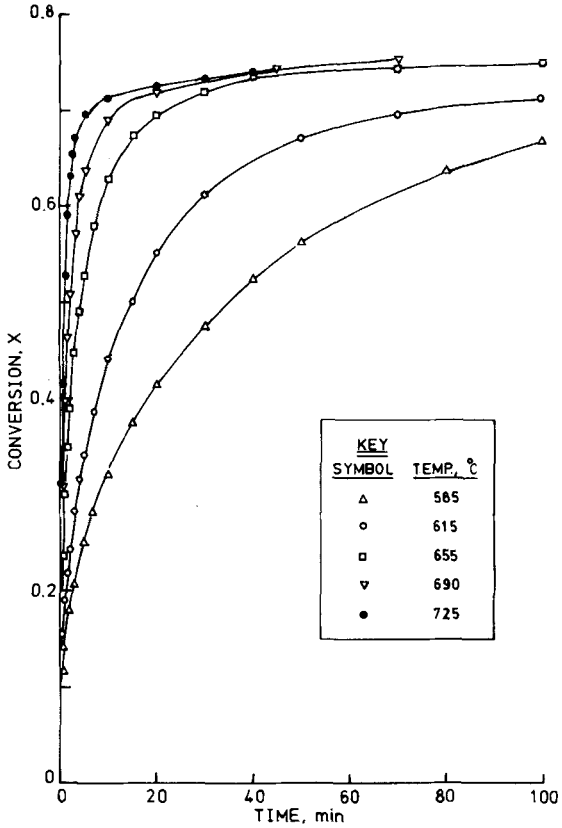

Figure 6. Effect of temperature on the reaction of 81 μm (−170 +200 mesh) particles reacted in a 42% CO_2-58% N_2 gas mixture. Calcine number 3, thermal history A.

which reduces exactly to $(1/2)\,(dX/dt)$ at low conversions. The result of such a test is shown as Figure 10, confirming the expected kinetic order for the growth stage.

Consistent with prior reports (Dedman and Owen, 1962; Nitsch, 1962) Figures 4, 5, and 7 show the slow second stage reaction rate to be independent of CO_2 partial pressure, but it should be noted that the CO_2 partial pressures used are far in excess of the equilibrium values for the CaO-CO_2-$CaCO_3$ system (Parkes, 1963; Kelley and Anderson, 1935). Very slight effects may be detected in Figures 5 and 7 in comparing changes in CO_2 level from 10% to 42% and 50%, respectively. In the runs at 963 K, the equilibrium CO_2 pressure is only 2.38 kPa. More easily detectable differences in rate were only produced with calcine number 2 using larger samples in experiments at 958 K and CO_2 levels below 35%. These results, which are reported in detail elsewhere (Bhatia, 1981), suggest that the second stage reaction rate is independent of CO_2 partial pressure, except close to equilibrium.

DISCUSSION

Incomplete Conversion

Since there is no significant effect of particle size over the range of conditions used in these experiments, the incomplete conversions observed are not attributable to surface pore closure as in other systems (Hartman and Coughlin, 1976; Bhatia and Perlmutter, 1981b). Instead the sharply attenuated rates that occur at conversions of 60 to 65% may be related to the effective closure of the small pores of a rather narrow size range, but not limited to the surface. After the small pores close uniformly throughout the particle, the larger pores of much smaller surface area continue the reaction but at a greatly reduced rate.

To support this argument by quantitative considerations, assume following Borgwardt (1970) and Hartman and Coughlin (1974) that conversion is proportional to loss in porosity at any time:

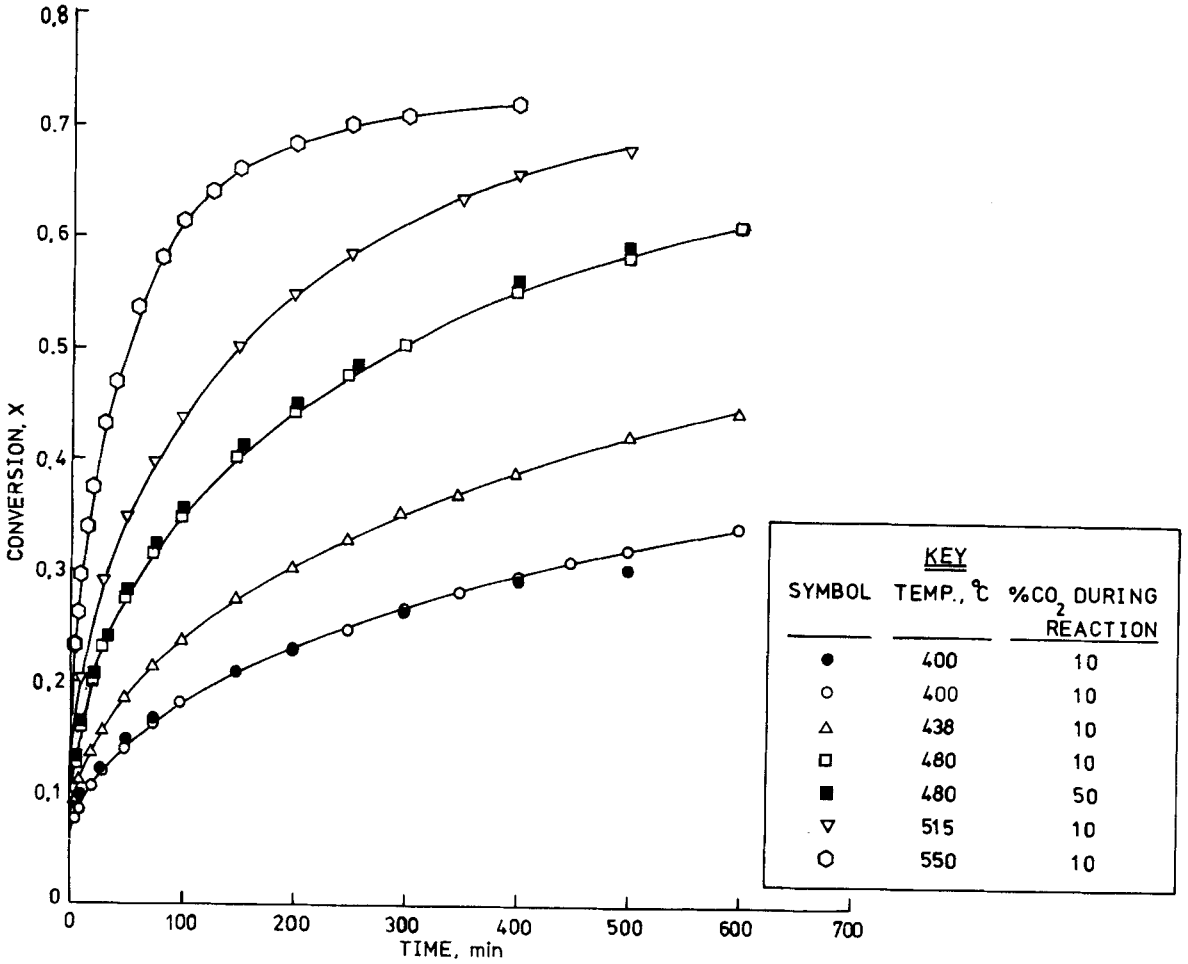

Figure 7. Effect of temperature on the reaction of 137 μm (−100 +120 mesh) particles. Calcine number 2, thermal history A.

$$X = \frac{\rho_T e_o}{(Z-1)} \tag{9}$$

where from Bhatia and Perlmutter (1981b):

$$Z = 1 + \frac{\rho(\alpha_C - \alpha_L)}{M} \tag{10}$$

For the system being considered:

α_C = 36.9 cm³/gmol, the molar volume of $CaCO_3$
α_L = 16.9 cm³/gmol, the molar volume of CaO
ρ = 3.23 g/cm³, the density of lime in the calcine

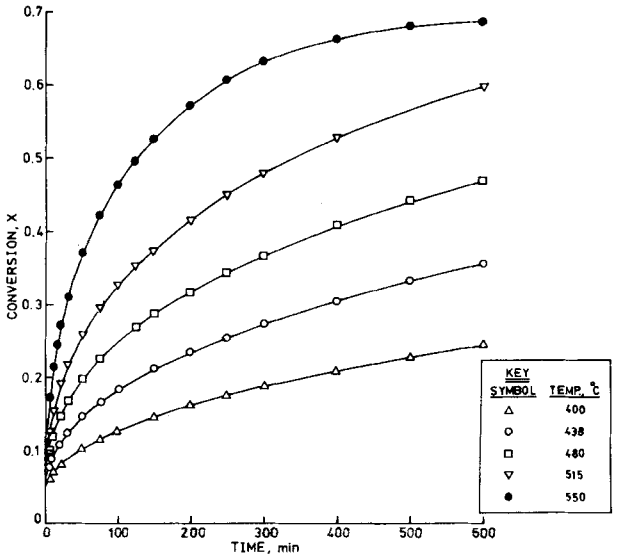

Figure 8. Effect of temperature on reaction of 137 μm (−100 +120 mesh) particles reacted in a 10% CO_2-90% N_2 gas mixture. Calcine number 3, thermal history A.

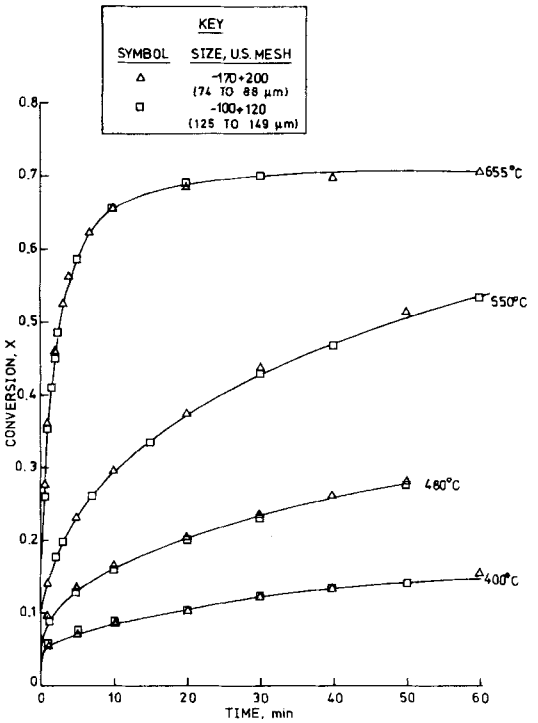

Figure 9. Effect of particle size for material calcined and reacted in a 10% CO_2-90% N_2 mixture. Calcine number 2, thermal history A.

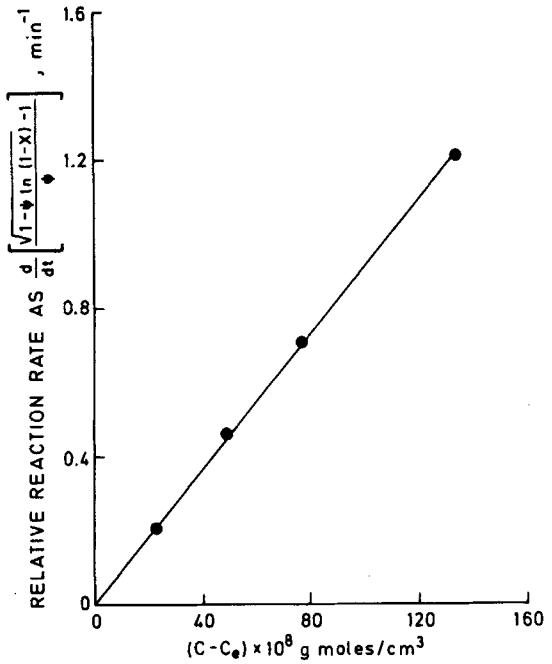

Figure 10. Effect of gas composition on reaction rate at 888°K, calcine number 1, thermal history B.

M = 56, the molecular weight of CaO
Z = 2.16 from Eq. 10
ρ_T = 3.32 g/cm^3, the crystal density of lime

Substituting these values in Eq. 9 gives

$$X = 2.86\, e_o \tag{11}$$

Following the argument that attributes the sharp slowing of reaction to the exhaustion of relatively small pores, this process would be expected to occur at conversion levels where e_o is the cumulative small pore volume. The data of Figure 1 show that about 0.25 cm^3/g of pore volume lies in pores of a relatively narrow size range for all the calcines, with the remainder in larger pores distributed over a much wider range. Setting e_o = 0.25 cm^3/g, Eq. 9 provides X = 0.71, in excellent agreement with the experimentally observed results.

Kinetic Parameter Estimation

The linear growth stages that appear in Figures 2 and 3 may be used to evaluate intrinsic kinetic parameters, since the intraparticle and transport resistances are insignificant under the conditions of study. Such estimates are presented in Table 3, based on data fits to Eq. 3 and the appropriate parameters taken from Table 2. The rate constant k_s does not exhibit a significant trend with changes in temperature, nor has it been affected by the additional cooling and reheating to which the materials that produced Figure 3 were subjected. The average value of k_s is found to be 0.0595 ± 0.0018 cm^4/gmol-s at the 95% level of confidence. The finding that the initial rapid reaction between 823 and 998 K has zero activation energy is consistent with the higher temperature (1,073 to 1,173 K) reports of Nitsch (1962) and Zawadzki and Bretsznajder (1935). The lack of activation for the growth reaction may also be expected from the reports of Zawadzki and Bretsznajder, and Cremer and Nitsch (1962) to the effect that the activation energy for the decomposition of $CaCO_3$ is the same as its heat of formation from CaO and CO_2.

Calculations using the rate constants estimated in this research (Bhatia, 1981) showed that no significant concentration or temperature gradients exist either in the particles or in the boundary layer surrounding them, under the conditions of the experiments. These results are in agreement with the experimental finding that particle size had no effect and justify the neglect of transport resistances in the evaluation of kinetic parameters.

TABLE 3. RATE CONSTANTS FOR THE LIME-CO_2 REACTION
CALCINE NUMBER 1

Run Number	Thermal History	Temp. K	Rate Constant k_s cm^4/gmol-s
0-6	A	998	0.0594
0-7	B	998	0.0571
0-1	A	998	0.0385
0-12	A	963	0.0592
0-16	B	963	0.0601
0-13	A	963	0.0424
0-11	A	928	0.0568
0-10	A	888	0.0631
0-9	A	858	0.0369
0-14	B	823	0.0614
*	A	888	0.0586

* Average of four runs shown in Figure 10.

Diffusion Parameter Estimation

If as suggested above the slower second stage of reaction is controlled by a product layer diffusion process that follows Eq. 8, the appropriate diffusivity may be estimated from the slope of a linear relation between the ratio $[\sqrt{1-\psi \ln(1-X)}-1]/\psi$ and the square-root of time. This expectation was confirmed by testing the data of Figures 4 to 8. As shown for example in Figures 11 and 12 for calcine number 3, the data follow the linear pattern to about 55 to 60% conversion. The deviations for low conversions reflect the rapid initial stage previously considered. Similar results were found for the other calcines.

The values of effective diffusivities for each of the calcines were computed from the linear slopes consistent with Eq. 8, together with the several physical parameters for the different solids taken from Table 2. Activation energies were obtained for the diffusion coefficients via the usual Arrhenius coordinates in Figure 13. Within a 95% confidence interval a value of 88.9 ± 3.7 kJ/mol represents all three calcines below 788 K, a result in agreement with that obtained for lime by Hashimoto (1961) from electrical conduction experiments. Above this temperature, the value increases

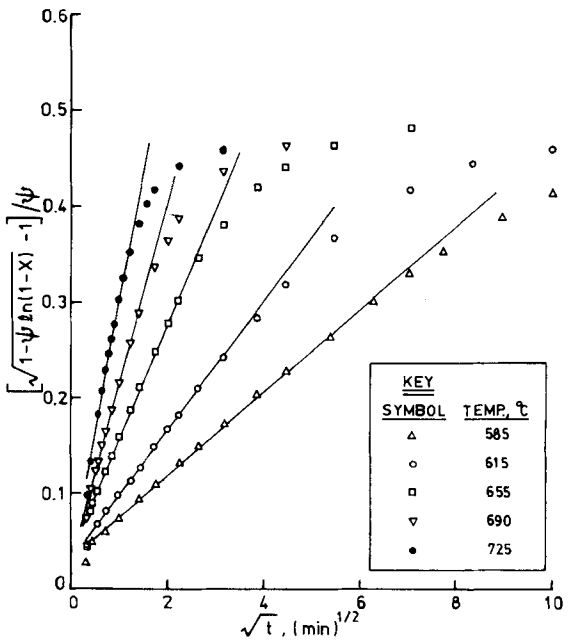

Figure 11. Data of Figure 6 plotted according to coordinates suggested by Eq. 8.

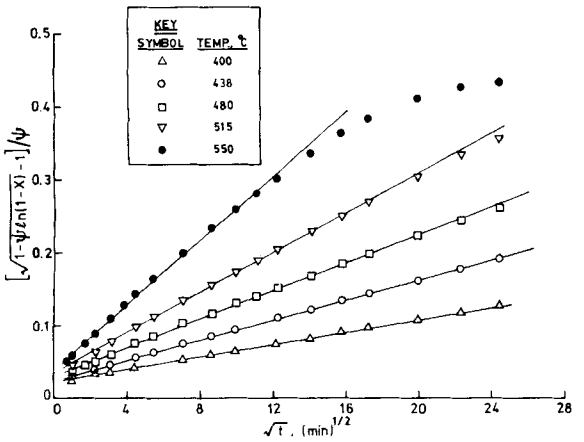

Figure 12. Data of Figure 8 plotted according to coordinates suggested by Eq. 8.

abruptly to 179.2 ± 7.0 kJ/mol, strongly suggesting a change in mechanism. A similar sharp change in activation energy for CO_2 exchange with $CaCO_3$ was found by Anderson (1969) between 788 and 823 K. It should be noted that the diffusivity is reduced by half when the calcining atmosphere includes CO_2 as the nitrogen diluent.

Alternatively, Eq. 7 could as well have been used to estimate the rate constant and diffusional parameter, but the limiting forms in Eqs. 3 and 8 are more convenient because the initial rapid stage is seen to be chemical reaction controlled and the slower second stage product layer, diffusion controlled. This relatively sudden transition from one regime to another is striking, since there is more usually a gradual transition from reaction to diffusion control with both mechanisms significant over a large conversion range. This peculiar sudden changeover observed in this reaction is discussed in the context of the reaction mechanism in the following section.

Reaction Mechanism

Several items of evidence point to the participation of a solid-state process in the chemistry being considered, in a manner somewhat analogous to the previously examined SO_2-lime reaction (Bhatia and Perlmutter, 1981b). First, the relatively low diffusivities in the product layer and the correspondingly large activation energies are inconsistent with a simple gas molecule diffusion. Further, the observed change in activation energy at 788 K is to be expected for a solid state process, since the Tammann temperature for $CaCO_3$ is about 800 K (Shewmon, 1963; Leclair, 1976). Finally, the agreement noted between these results and those of Hashimoto strongly suggests that the diffusion process proceeds by a mechanism similar to that taking place during conduction in $CaCO_3$. Anderson (1969), who used isotopic exchange between CO_2 and $CaCO_3$ to study diffusion, reported that 50-fold reductions in diffusivity could be achieved by annealing $CaCO_3$ and attributed this to changes in defect structure. Such variations in diffusivity are consistent with those found in this study between the calcines produced under nitrogen or N_2-CO_2 mixed atmospheres, since crystallinity differences between these materials were also observed.

Since the Ca^{+2} and CO_3^{-2} ions are predominant in $CaCO_3$ they are likely candidates for ionic motion. Measurements by Arnekar and Chaure (1970) provide a value for diffusivity of Ca^{+2} in $CaCO_3$ at 573 K of 4.9×10^{-15} m^2/s. This result is six orders of magnitude larger than that calculated from an extrapolation of the Hashimoto conduction result; thus the diffusing species is probably CO_3^{-2} in this temperature range.

If CO_3^{-2} is accepted as the mobile species in ionic conduction through $CaCO_3$, then one must postulate a counter-current motion of a negatively charged species during the reaction process to maintain electroneutrality in the product layer. In the system

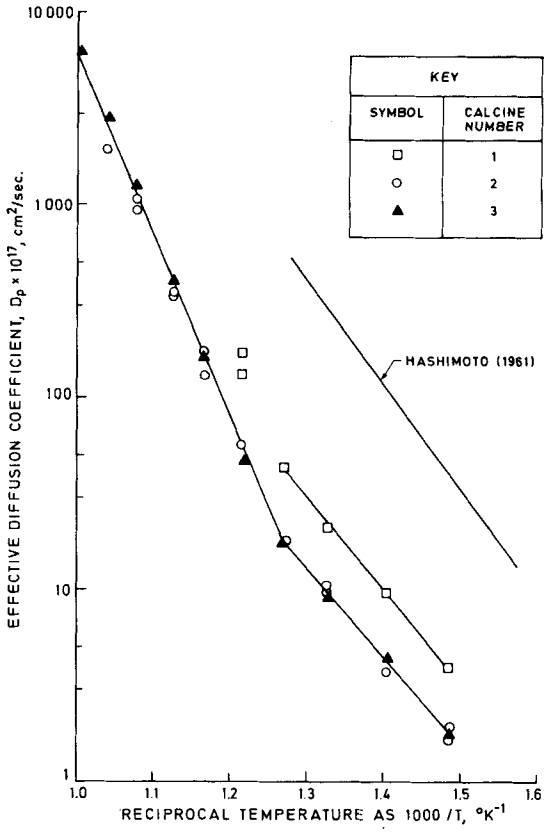

Figure 13. Comparison of effective product layer diffusivities for various calcines.

CaO-$CaCO_3$-CO_2 the most probable candidate is O^{-2}. A plausible mechanism for the reaction may thus be written as

$$CO_3^{-2} + CaO \rightarrow CaCO_3 + O^{-2}$$

at the CaO-$CaCO_3$ interface, and

$$CO_2\,(g) \leftrightharpoons (CO_2)_{ads}$$

$$(CO_2)_{ads} + O^{-2} \rightarrow CO_3^{-2}$$

at the pore surface. In the experiments conducted in this research CO_2 concentrations were far from equilibrium, and the reaction was found to be independent of gas concentration. In terms of the above mechanism this must imply that the adsorbed gas concentration had reached its saturation value. In addition, the observed parabolic correlation is in agreement with a diffusion controlled process, suggesting that the above ionic reactions at the two surfaces are at equilibrium.

An alternative diffusion mechanism seems more likely to apply in the elevated temperature range over 788 K, where the activation energy of 179.2 kJ/mol agrees closely with the 178.5 kJ/mol heat of decomposition of $CaCO_3$. A possible pathway for effective CO_2 diffusion could arise from sequential decompositions of carbonate ions in the calcium carbonate layer. A CO_3^{-2} ion momentarily decomposes to give carbon dioxide and an oxygen ion. The carbon dioxide molecule than moves to a neighbouring similarly vacated site, while another carbon dioxide so produced elsewhere moves to take its place and reform the carbonate ion. The carbon dioxide molecule thus diffuses site to site through the product layer, ultimately reacting at the CaO-$CaCO_3$ interface.

The existence of the first stage chemically controlled reaction is compatible with either of the two mechanisms hypothesized above if the initial product layer has an extremely high diffusivity, causing reaction at the CaO-$CaCO_3$ interface to control the overall process. This argument is supported by several published investigations of the isotopic exchange between carbon dioxide and calcium carbonate. In particular Haul et al. (1953), Haul and Stein (1955), and Anderson (1969) all reported an initial rapid exchange

followed by a slower diffusion controlled step. This is generally regarded as due to anomalies such as channels and grain boundaries in the surface layer of $CaCO_3$, which promote diffusion. In this view, the relatively rapid transition observed from the initial reaction to the second stage represents the formation of a more compact layer with a much lower diffusivity.

ACKNOWLEDGMENT

This research was funded by the National Science Foundation under Grant No. CPE-8000291.

NOTATION

a,b = stoichiometric coefficients
C = concentration of CO_2
C_e = equilibrium concentration of CO_2
C_s = concentration of diffusing species on pore surface
D = effective product layer diffusivity
D_p = $bMDC_s/a\rho$
e_o = loss in pore volume per unit mass, during reaction
k_x = effective reaction rate constant
k_s = rate constant for surface reaction
L_o = initial total length of pore system per unit volume
M = molecular weight of CaO
r = pore radius
S_o = initial surface area per unit volume
t = time
$v_o(r)$ = pore volume distribution function
X = conversion
Z = ratio of volume of solid phase after reaction to that before reaction

Greek Letters

α_L = molar volume of CaO
α_C = molar volume of $CaCO_3$
β = $\dfrac{2k_s a\rho(1-\epsilon_o)}{bMDS_o}$
ϵ_o = initial porosity
ψ = $\dfrac{4\pi Lo(1-\epsilon_o)}{S_\rho^2}$, structural parameter
ρ = mass of CaO per unit volume of solid phase
ρ_T = crystal density of lime

LITERATURE CITED

Anderson, T. F., "Self-Diffusion of Carbon and Oxygen in Calcite by Isotopic Exchange with Carbon Dioxide," *J. Geophysical Res.*, **74,** 3918 (1969).

Arnikar, H. J., and B. D. Chaure, *Proc. 1st Chem. Symp.*, Chandigarh, India, **2,** 144 (1970).

Baker, R., "The Reversibility of the Reaction $CaCO_3 \rightleftharpoons CaO + CO_2$," *J. Appl. Chem. Biotechnol.*, **23,** 733 (1973).

———, "The Reactivity of Calcium Oxide Toward Carbon Dioxide and Its Use for Energy Storage," *ibid.*, **24,** 221 (1974).

Beruto, D., and A. W. Searcy, "Use of the Langmuir Method for Kinetic Studies of Decomposition Reactions: Calcite ($CaCO_3$)," *J. Chem. Soc., Faraday Trans., I,* **70,** 2145 (1974).

———, "Calcium Oxides of High Reactivity," *Nature*, **263,** 221 (1976).

Bhatia, S. K., "The Effect of Pore Structure on the Kinetics of Fluid-Solid Reactions," Ph.D. Dissertation, University of Pennsylvania (1981).

Bhatia, S. K., and D. D. Perlmutter, "A Random Pore Model for Fluid-Solid Reactions: I. Isothermal, Kinetic Control," *AIChE J.*, **26,** 379 (1980).

Bhatia, S. K., and D. D. Perlmutter, "A Random Pore Model for Fluid-Solid Reactions Part II. Diffusion and Transport Effects," *AIChE J.*, **27,** 247 (1981a).

Bhatia, S. K., and D. D. Perlmutter, "The Effect of Pore Structure on Fluid-Solid Reactions: Application to the SO_2-Lime Reactions," *AIChE J.*, **27,** 226 (1981b).

Borgwardt, R. H., "Kinetics of Reaction of SO_2 with Calcined Limestone," *Environ. Sci. Technol.*, **4,** 59 (1970).

Borgwardt, R. H. and R. D. Harvey, "Properties of Carbonate Rocks Related to SO_2 Reactivity," *Environ. Sci. Technol.*, **6,** 350 (1972).

Cremer, Von E., and W. Nitsch, "Über die Geschwindigkeit der $CaCO_3$-Zersetzung in Abhängigkeit Vom CO_2 Druck," *Z. Electrochem.*, **66,** 697 (1962).

Dedman, A. J., and A. J. Owens, "Calcium Cyanamide Synthesis. Part 4—The Reaction $CaO + CO_2 = CaCO_3$," *Trans. Faraday Soc.*, **58,** 2027 (1962).

Gavalas, G. R., "A Random Capillary Model with Application to Char Gasification at Chemically Controlled Rates," *AIChE J.*, **26,** 577 (1980).

Hartman, M., and R. W. Coughlin, "Reaction of Sulfur Dioxide with Limestone and the Influence of Pore Structure," *Ind. Eng. Chem. Proc. Des. Dev.*, **13,** 248 (1974).

Hartman, M., and R. W. Couglin, "Reaction of Sulfur Dioxide with Limestones and the Grain Model," *AIChE J.*, **22,** 490 (1976).

Hashimoto, H., "Thermal Decomposition of Calcium Carbonate (I)—Annealing Process and Electric Conductivity," *Kogyo Kagaku Zasshi*, **64,** 250 (1961).

Haul, R. A. W., and L. H. Stein, "Diffusion in Calcite Crystals on the Basis of Isotopic Exchange with Carbon Dioxide," *Trans. Faraday Soc.*, **51,** 1280 (1955).

Haul, R. A. W., L. H. Stein, and J. W. L. DeVilliers, "Exchange of Carbon-13 Dioxide Between Calcite Crystals and Gaseous Carbon Dioxides," *Nature*, **171,** 619 (1953).

Hyatt, E. P., I. B. Cutler, and M. E. Wadsworth, "Calcium Carbonate Decomposition in Carbon Dioxide Atmosphere," *J. Am. Ceram. Soc.*, **41,** 70 (1958).

Kelley, K. K., and C. T. Anderson, "Data on Theoretical Metallurgy: IV Metal Carbonates-Correlations and Applications of Thermodynamic Properties," *U.S. Bur. Mines Bull.*, No. 384 (1935).

LeClaire, A. D., "Duffusion," *Treatise on Solid State Chemistry*, N. B. Hannay, ed., **4,** 1, Plenum Press, New York, (1976).

McClellan, G. H., and J. L. Eades, "The Textural Evolution of Limestone Calcines," *The Reaction Parameters of Lime*, ASTM Special Tech. Publ., **472,** 209 (1970).

Mullins, R. C., and J. D. Hatfield, "Effects of Calcination Conditions on the Properties of Lime," *The Reaction Parameters of Lime*, ASTM Special Tech. Publ., **472,** 117 (1970).

Nitsch, Von W., "Über die Druckabhängigkeit der $CaCO_3$-Bildung aus dem Oxyd," *Z. Elektrochem.*, **66,** 703 (1962).

Parkes, G. D., *Mellor's Modern Inorganic Chemistry*, Longmans, Green and Co., London (1963).

Rao, C. N. R., S. R. Yoganarasimhan, and M. P. Lewis, "Exothermic Reactions Due to Annealing of Defects in Oxide Lattices: Study of the Decomposition of Carbonates," *Can. J. Chem.*, **38,** 2359 (1960).

Searcy, A. W., and D. Beruto, "Kinetics of Endothermic Decomposition Reactions. I. Steady State Chemical Steps," *J. Phys. Chem.*, **80,** 425 (1976).

Shewmon, P. G., *Diffusion in Solids*, McGraw Hill, New York (1963).

Szekely, J., J. W. Evans, and H. Y. Sohn, *Gas-Solid Reactions*, Academic Press, London (1976).

Ulerich, N. H., E. P. O'Neill, and D. L. Keairns, "A Thermogravimetric Study of the Effect of Pore Volume-Pore Size Distribution on the Sulfation of Calcined Limestone," *Thermochimica Acta*, **26,** 269 (1978).

Young, D. A., *Decomposition of Solids*, Pergamon Press, Oxford (1966).

Zawadzki, J., "The Effect of Temperature on the Rate of Reaction," *Disc. Faraday Soc.*, **8,** 151 (1950).

Zawadzki, J., and S. Bretsznajder, "Über das Temperaturinkrement der Reaktionsgeschwindigkeit bei Reaktionen vom Typus $A_{fest} = B_{fest} + C_{gas}$," *Z. Electrochem.*, **41,** 215 (1935).

Manuscript received July 24, 1981; revision received March 18, and accepted March 23, 1982.